



## Bistriazine-based streptocyanines. Preparation, structural determination and optoelectronic properties



Fernando León <sup>a, b</sup>, Patricia Elizalde <sup>a, b</sup>, Pilar Prieto <sup>a</sup>, Ana Sánchez-Migallón <sup>a, \*\*</sup>, Antonio M. Rodríguez <sup>a, c</sup>, Antonio de la Hoz <sup>a, \*</sup>

<sup>a</sup> Departamento de Química Orgánica, Facultad de Ciencias y Tecnologías Químicas, Universidad de Castilla-La Mancha, 13071 Ciudad Real, Spain

<sup>b</sup> Departamento de Química Orgánica, Universidad Nacional Autónoma de México, Facultad de Química, 04510 México, Distrito Federal, Mexico

<sup>c</sup> Department of Chemical Sciences, University of Naples Federico II, 80126 Naples, Italy

### ARTICLE INFO

#### Article history:

Received 4 January 2016

Received in revised form

1 April 2016

Accepted 6 April 2016

Available online 7 April 2016

#### Keywords:

Triazine

Streptocyanine

Computational calculations

DNMR

Luminescence

Microwave

### ABSTRACT

A series of bistriazine-based streptocyanines has been selectively prepared. A variety of substituents has been introduced into the triazine ring with *p*-phenylenediamine as a conjugated spacer between the triazine and the streptocyanine moieties. Fukui indices have been used to explain the different sequential reactivity of the chlorine atoms in the triazine ring. 1D- and 2D-DNMR spectroscopy and computational calculations have been carried out to explain the dynamic behavior of these complex systems, which can be explained by the presence of a Cl ... H bond. This method was used to build conjugated systems and to show the interaction between the triazine part, the spacer, and the streptocyanine moiety. A study of the optoelectronic properties has been performed by UV–vis and fluorescence spectroscopy. Streptocyanine-based bistriazines are violet-blue emitters and large Stokes shifts of more than 6000 cm<sup>-1</sup> were observed. The title compounds showed interesting properties which have potential for use in optoelectronic devices.

© 2016 Elsevier Ltd. All rights reserved.

## 1. Introduction

$\pi$ -Conjugated molecular structures are among the most investigated systems in the field of molecular materials due to their interesting optical and electronic properties [1]. However, the efficiency of optoelectronic devices based on  $\pi$ -conjugated systems is not only highly depended on the chemical structure but also on the supramolecular aggregation. Therefore, the construction of  $\pi$ -conjugated assemblies with controlled morphology and the desired properties is crucial for the fabrication of the aforementioned devices [2].

The choice of a good material for a specific application is hindered by the complex structure–property relationship. An interesting approach to tune the absorption in  $\pi$ -conjugated systems is the incorporation of electron donor (D) and electron acceptor (A) moieties in the molecular design [1,3,4]. Linear and star-shaped systems are among the most interesting  $\pi$ -conjugated materials

that contain D and A groups.

Triazine derivatives have been used for the construction of star-shaped derivatives. Some examples of star-shaped triazine derivatives with a D– $\pi$ –A [5] or D– $\pi$ –A– $\pi$ –D– $\pi$ –A [6] electronic arrangement have found applications in solar cells [7], magnetic materials [8], and blue-luminescent OLEDs [9]. In particular, the later type of system has been shown to promote electron transport, and the derivatives synthesized according to this design exhibit large Stokes shifts, high thermal stability, and solvatochromism [10].  $\pi$ -Conjugated systems that contain only one triazine ring have been investigated for many years [11,12] but bistriazines have received much less attention [13].

We recently described the preparation of mono- and bistriazines with phenylenediamine spacers with interesting optoelectronic properties. The electronic properties depend on the solvent and, in methanol, large bathochromic shifts and high quantum yields were observed [14].

According to the approach outlined above, we planned the preparation of bistriazines with a streptocyanine spacer. Streptocyanines are highly conjugated dyes with extended  $\pi$ -systems. These dyes show absorptions at long wavelengths and have high molar absorptivities. Streptocyanines with Donor and Acceptor

\* Corresponding author.

\*\* Corresponding author.

E-mail addresses: [Ana.Smigallon@uclm.es](mailto:Ana.Smigallon@uclm.es) (A. Sánchez-Migallón), [Antonio.Hoz@uclm.es](mailto:Antonio.Hoz@uclm.es) (A. de la Hoz).

groups have been used as Push-Pull systems [15]. These materials are classified as streptopolymethines, cationic hemicyanines, anionic streptopolymethine oxonols, neutral merocyanines, and cyanines based on zwitterionic squarines. Cyanines have found applications in Dye Sensitized Solar Cells (DSSC) [7] as donor- $\pi$  bridge-acceptor systems and, in some cases, they show impressive efficiency [16]. Many of these compounds are either blue emitters or absorb in the NIR region [17].

Kawamura [11] synthesized a squarylium-triazine dyad as a photoradical generator that absorbs strongly in the red region and undergoes an intramolecular photodissociative electron-transfer reaction.

The aim of this research is the preparation of a new series of bistriazine-based streptocyanines in order to show the influence of this remarkable  $\pi$ -deficient heterocycle, that can show all possible supramolecular interactions, on the optoelectronic properties of streptocyanine dyes.

## 2. Results and discussion

### 2.1. Synthesis of streptocyanines 7

The synthesis of the streptocyanines was planned in three steps, starting with cyanuric chloride (**1**), disubstitution with aliphatic and aromatic amines (**2**), reaction with *p*-phenylene diamine (**4**) to give the monofunctional product (**5**) and finally reaction with 3-chloro-*N,N,N',N'*-tetramethyl-1,5-diaza-1,3-pentadienium hexafluorophosphate (**6**) (Scheme 1).

Starting with cyanuric chloride it is possible to replace sequentially the three chloro-substituents with nucleophiles [18]. The first substitution can be performed at 0 °C, the second one at room temperature while the third substitution requires higher temperatures, usually under reflux in an appropriate solvent.

The Fukui indices in cyanuric chloride and the mono- and disubstituted compounds were determined computationally in order to explain the different reaction conditions in the sequential substitution of the chloro-substituents in cyanuric chloride. In brief, Fukui indices provide information about which atoms in a molecule have a higher tendency to either lose or accept an electron.

In chemistry this information is used to identify the positions that are more prone to undergo nucleophilic or electrophilic attack. Therefore, in an attempt to rationalize the different reactivities of the chloro-substituents in cyanuric chloride, the condensed Fukui function for the nucleophilic attack ( $f_A^+$ ) [19] on monosubstituted and disubstituted derivatives was calculated at the reactive carbon atoms of the triazine ring within the framework of Density Functional Theory (DFT) [20], employing the functional B3LYP [21] and 6-311 + G(d,p) [22] as the basis set. The electrophilicity of an atom A in a molecule M (of N electrons) was calculated using the

following equation:

$$f_A^+ = P_A(N+1) - P_A(N)$$

Where P stands for the population of atom A in a molecule M. The calculated values are collected in Table 1.

The Fukui indices confirm that increased substitution of the triazine ring results in a decrease in the electrophilic character that hinders nucleophilic substitution in the carbon atoms. For this reason, the calculated outcomes represent a straightforward method to interpret the selectivity observed.

### 2.2. Disubstituted triazines

The synthesis of disubstituted triazines was performed by double substitution of cyanuric chloride according to the procedure of Kolmatov [23] for aromatic amines. The reaction conditions and yields were very dependent on the basicity of the amine. For strongly basic amines an acetic acid/sodium acetate buffer was used but for amines with low basicity only acetic acid was required (Table 2). *p*-Anisidine, 1-naphthylamine and diphenylamine were selected because they show interesting properties as fluorophores in fluorescence spectroscopy [24].

The reaction with diphenylamine ( $pK_a = 0.79$ ) required the use of acetic acid and 60 h to produce the monosubstituted product **3c'** in good yield (85%). The use of solvent-free conditions at high temperatures [25] enabled triple substitution to give **3c''** in 74% yield. Finally, preparation of the desired 6-chloro-4,6-bis(*N,N*-diphenylamino)-1,3,5-triazine (**3c**) could be performed in basic conditions (Diisopropylethylamine, DIPEA) under reflux in di(*n*-butyl)ether (Scheme 2).

### 2.3. Introduction of the spacer, *p*-phenylenediamine (**4**)

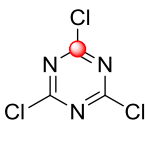
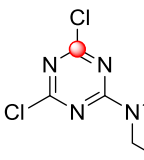
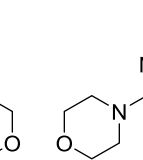
The third substitution, which required harsher conditions, was performed under microwave irradiation in the minimum amount of DMSO (Table 3), with simple purification procedures to give compounds **5** in excellent yields [14].

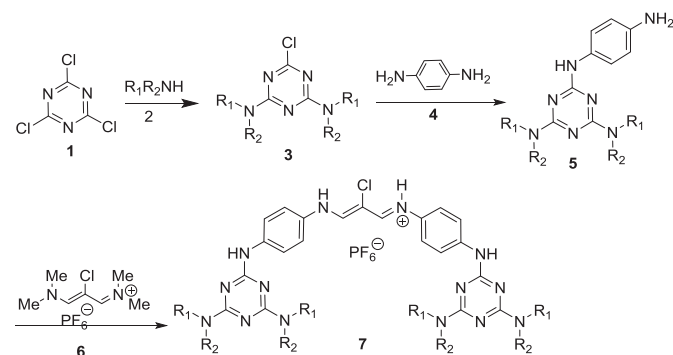
### 2.4. Preparation of streptocyanines 7

Finally, the synthesis of the streptocyanines was performed by reaction of triazines **5** with 3-chloro-*N,N,N',N'*-tetramethyl-1,5-diaza-1,3-pentadienium hexafluorophosphate (**6**) [26] in ethanol under reflux (Table 4).

The new compounds were characterized by spectroscopic methods, particularly MALDI-TOF mass spectrometry and NMR spectroscopy. The most characteristic signals in the  $^1\text{H}$ - and  $^{13}\text{C}$ -NMR spectra of compounds **7** are listed in Table 5. These dimeric systems show complex NMR spectra that are consistent with the structures and also with the wide range of dynamic processes that these compounds undergo. Some NMR spectra were recorded at 353 K because broad signals were observed for most compounds at

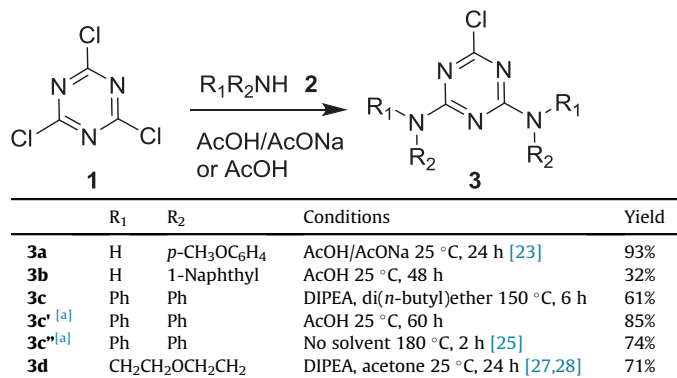
**Table 1**  
Fukui indices ( $f_A^+$ ) of the highlighted atom.

		
$f_A^+ = 0.065$	$f_A^+ = 0.048$	$f_A^+ = 0.039$

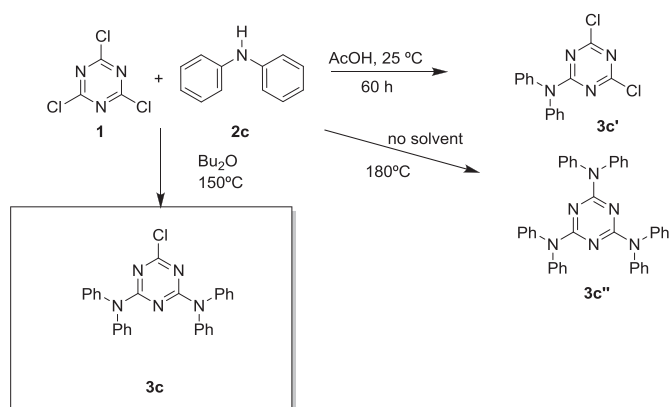


**Scheme 1.** Synthesis of dimeric triazines with a streptocyanine spacer.

**Table 2**  
Reaction of cyanuric acid with aromatic and aliphatic amines.



<sup>a</sup> See Scheme 2 for these structures.



**Scheme 2.** Reaction of cyanuric chloride (1) with diphenylamine (2c).

**Table 3**  
Reaction of disubstituted triazines 3 with *p*-phenylenediamine (4).

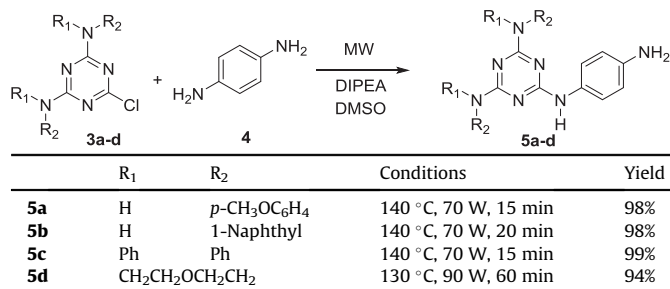


**Table 4**  
Preparation of dimeric streptocyanines 7.

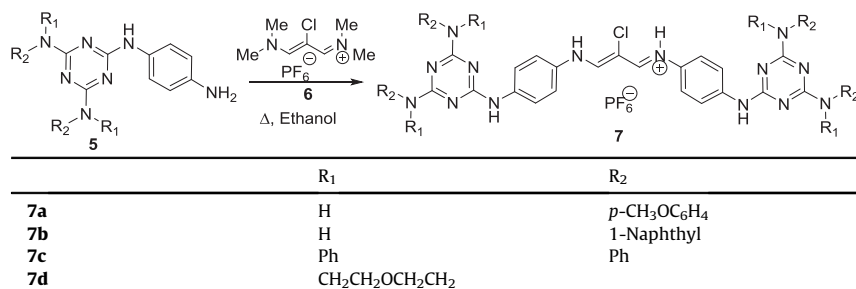
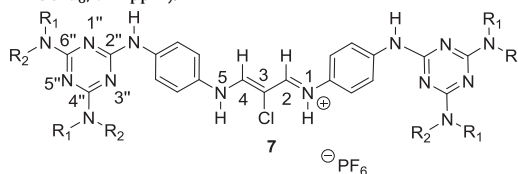


**Table 5**  
Characteristic signals in the <sup>1</sup>H- and <sup>13</sup>C-NMR spectra of compounds 7 (solvent DMSO-d<sub>6</sub>, δ in ppm).



a R<sub>1</sub> = H, R<sub>2</sub> = *p*-CH<sub>3</sub>OC<sub>6</sub>H<sub>4</sub>

b R<sub>1</sub> = H, R<sub>2</sub> = 1-Naphthyl

c R<sub>1</sub> = R<sub>2</sub> = Ph

d R<sub>1</sub> = R<sub>2</sub> = CH<sub>2</sub>CH<sub>2</sub>OCH<sub>2</sub>CH<sub>2</sub>

	H-2,4	NH-2''	NH-4'',6''	NH-1,5	C-3	C-2''	C-4'',6''
<b>7a</b>	8.24	8.99	9.09	[a]	94.27	163.87	163.99
<b>7b</b>	8.99	7.20	9.13	[a]	98.00	164.06	166.03
<b>7c</b>	8.17	6.81	—	9.1	98.08	161.57	163.28
<b>7d</b>	8.01, 8.26	9.02, 9.09	—	9.0	106.07	163.57	164.54

<sup>a</sup> Not observed.

298 K. This broadening is especially significant in the <sup>13</sup>C-NMR spectra and some signals were not observed clearly even at high temperatures. Due to the low solubility of the streptocyanines NMR spectra were recorded in DMSO, this produced some decomposition of the diimines to the amine and enamine, when long experiments were required.

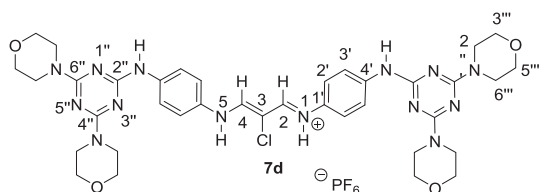
The <sup>1</sup>H-NMR spectra show the presence of three different NH groups and the H-2,4 signal at low field. In the <sup>13</sup>C-NMR spectra, the most characteristic signals are an upfield signal for C-3 of the streptocyanine chain (δ ~ 100) and two different signals for the carbon atoms of the triazine ring. Signals of C-2,4 are hardly observed at 150 ppm as broad signals due to a dynamic process.

Protons 2 and 4 of the dienic system are equivalent by mesomerism and they appear as broad signals at 298 K. In compound **7d**, however, two signals are observed (one as a singlet and the second as a doublet) and the signals of the *p*-phenylene group are also split.

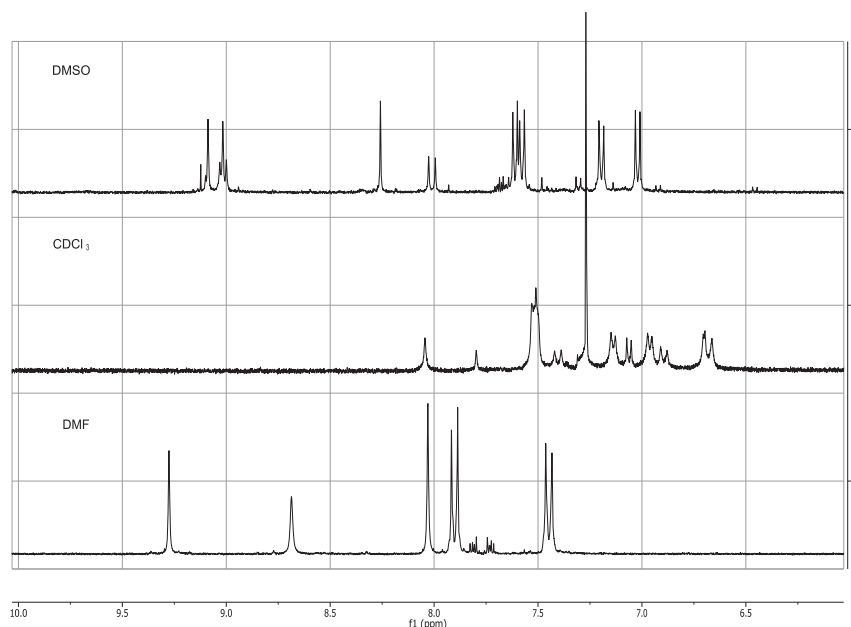
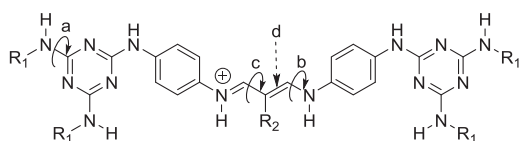
The NMR data and spectra of **7d** in different solvents and different temperatures are shown in Table 6 and Fig. 1. It is remarkable that splitting is observed at 298 K in DMSO-d<sub>6</sub> and CDCl<sub>3</sub> but not in solution in DMF-d<sub>7</sub>, for which splitting is only observed at lower temperature (233 K).

The synthesized compounds can show a great variety of isomers due to the occurrence of different processes such as restricted rotation and configurational isomerism (Fig. 2).

It is known that aminotriazines show restricted rotation around the aminotriazine bond that leads to four possible isomers [27], and a similar process is observed in 1,5-diazapentadiene systems to give three isomers [26]. These processes have been studied by us and others and the free energy of activation has been determined by variable temperature NMR experiments [28]. Finally, *s-cis/s-trans*

**Table 6**<sup>1</sup>H-NMR data for compound **7d** in DMSO-d<sub>6</sub>, CDCl<sub>3</sub>, and DMF-d<sub>7</sub> (δ, in ppm, J in Hz).

Solvent	T (K)	N-CH <sub>2</sub>	H-2',6'	H-3',5'	H-2,4	NH-1,5	NH
DMSO	298	3.60	7.02	7.61	8.01 d J = 12.7	9.01 d J = 12.7	9.02
		3.67	7.19	7.58	8.26 s		9.09
CDCl <sub>3</sub>	298	3.66	6.94	7.51	7.39 d J = 12.7	6.88 d J = 12.7	6.65
		3.71	7.13		8.04 s		6.69
DMF	298	3.70	7.44	7.90	8.69		9.28
		3.76					
DMF	353	3.71	7.23	7.76	8.18		8.69
		3.77					
DMF	233	3.66	7.15	7.84	8.35 d J = 11.6		9.58
			7.45		8.4 s		9.64

**Fig. 1.** <sup>1</sup>H-NMR spectra of compound **7d** in DMSO-d<sub>6</sub>, CDCl<sub>3</sub>, and DMF-d<sub>7</sub> at 298 K.

a,b: Rotation of the C-N bond  
 c: s-cis/s-trans isomerization  
 d: Z/E isomerization

**Fig. 2.** Isomers produced by rotation and isomerization.

and Z/E isomerism are possible in the diene system of the streptocyanine moiety [29]. As a consequence, up to 72 isomers, rotamers, and configurational isomers are possible.

However, the different multiplicities of the H-2,4 signals (d and s) cannot be explained by these kinetic processes. The integral of the split signals indicates the presence of a 1:1 ratio in all solvents and this situation is unlikely to occur with two rotamers or isomers

with different stabilities (Table 6 and Fig. 1). This observation prompted us to study the origin of this result by DNMR experiments and computational calculations.

The coalescence temperature (270 K) and the chemical shift in the slow process (233 K) were determined from <sup>1</sup>H-NMR spectra of samples in DMF. A Free Energy of Activation of 12.9 kcal mol<sup>-1</sup> was calculated according to Sandström (Equation S1) [30]. However, similar experiments carried out in DMSO and CDCl<sub>3</sub> did not lead to coalescence of the NH groups. As a consequence, thermodynamic parameters for the rotation process were determined by 2D-EXSY experiments at 298 K, i.e., the temperature of a slow process, in both solvents. Rate constants were deduced according equation S2 and Free Energies of Activation were calculated from the rate constants according to Sandström [30] (Equation S3). The values obtained were 17.48 kcal mol<sup>-1</sup> in CDCl<sub>3</sub> (Fig. 3) and 17.65 kcal mol<sup>-1</sup> in DMSO-d<sub>6</sub>. It is remarkable that the doublet at δ 7.39 exchanges with the singlet at δ 8.04 ppm in CDCl<sub>3</sub>.

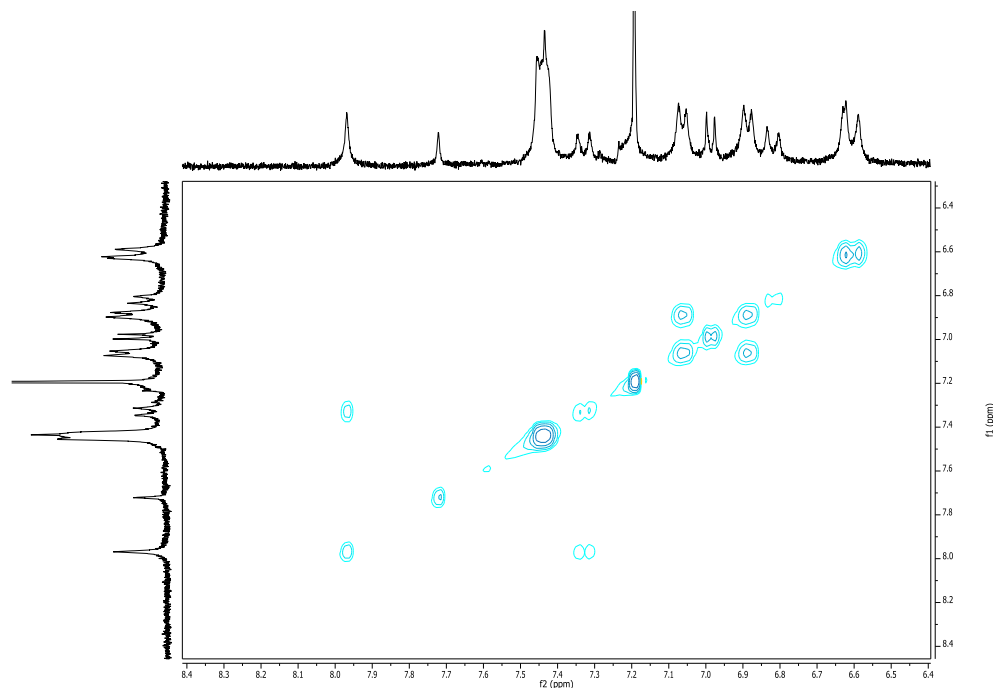


Fig. 3. 2D-EXSY ( $t_m = 1$  s) of compound **7d** in  $\text{CDCl}_3$  at 298 K.

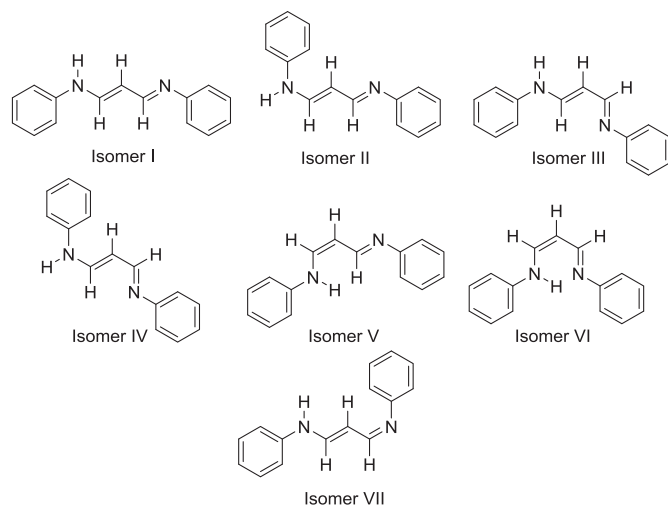


Fig. 4. Selected isomers of 1,5-diphenyl-1,5-diaza-2,3-pentadiene that were analyzed.

**Table 7**  
Relative energies of isomers I–VII in the gas phase and in solution.

Isomer	Energy ( $\text{kcal mol}^{-1}$ )		
	Gas phase	Solution ( $\text{CHCl}_3$ )	Solution (DMSO)
I	5.60	3.39	2.44
II	8.31	5.94	4.91
III	6.75	5.17	4.49
IV	9.30	7.66	7.00
V	7.90	6.03	5.14
VI	0.00	0.00	0.00
VII	8.27	5.99	5.07

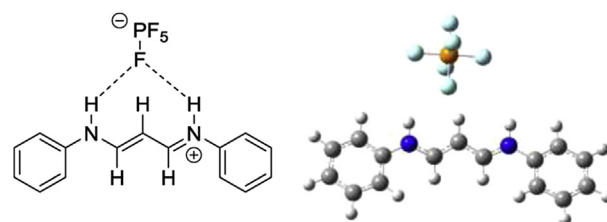


Fig. 5. Most stable structure of isomer I (hexafluorophosphate) in DMSO.

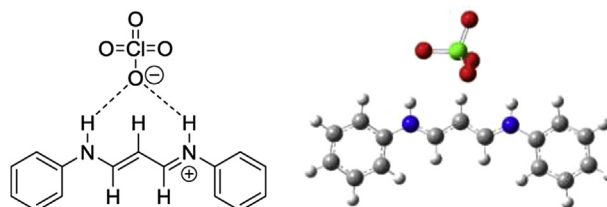


Fig. 6. Most stable structure of isomer I (perchlorate) in DMSO.

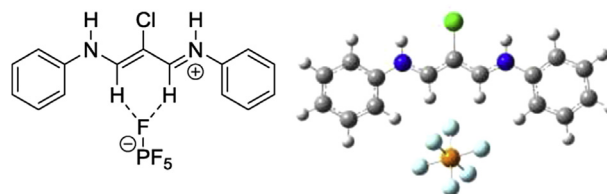
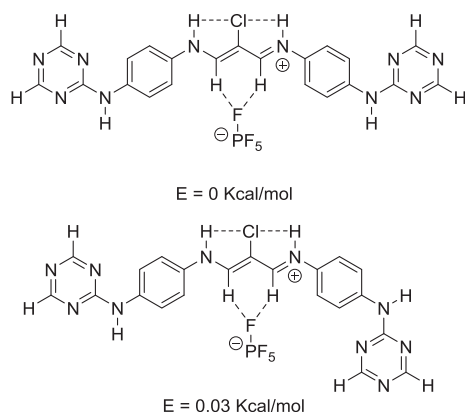


Fig. 7. Most stable structure of isomer I with a chlorine atom (hexafluorophosphate) in DMSO.

## 2.5. Computational calculations

A computational study of bistriazines **7** was carried out in order

to determine the main isomers and to compare the theoretical results with those obtained by NMR spectroscopy. Calculations were performed using B3LYP/6-31G(d,p) and the Density



**Fig. 8.** Rotamers obtained upon the introduction of the triazine moiety. Relative energy (kcal mol<sup>-1</sup>).

Functional Theory (DFT) in the gas phase and in solution (CHCl<sub>3</sub> and DMSO). In solution, Self-Consistent Reaction Field (SRCF) models for solvation were used. These continuum models consider the solvent as a continuum, dielectric, and polarizable medium and the solute is included in a cavity. This continuum is characterized by the dielectric constant ( $\epsilon$ ) of the solvent. In this case the Polarizable Continuum Model (PCM) was employed [31].

A stepwise optimization was carried out in order to simplify the calculations. First, we analyzed the central 1,5-diphenyl-1,5-diazapentadiene nucleus. In this case, we have chosen seven isomers from the sixteen possibilities, we have discarded the more congested isomers (Fig. 4). The results obtained are collected in Table 7. Then we proceeded to study the protonated species. Finally, we introduced sequentially the rest of the molecule, i.e., chlorine atom, triazine rings, and substituents.

The most stable isomer, both in the gas phase and in solution, is isomer **VI** and this stability is due to the formation of an intramolecular hydrogen bond (N ... H distance 1.93 Å). Isomer **I** is the second most stable isomer in DMSO and CHCl<sub>3</sub>, with a difference of 2.44 and 3.39 kcal mol<sup>-1</sup> respectively with respect to **VI**.

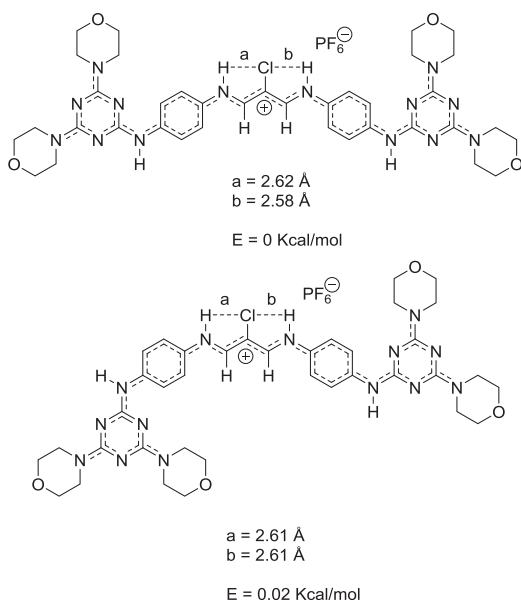
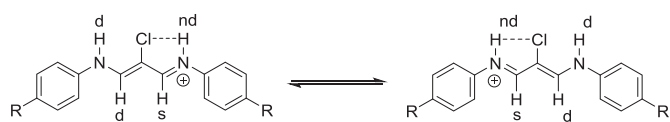


**Fig. 9.** Most stable isomers of compound **7d**. Relative energy (kcal mol<sup>-1</sup>) and hydrogen bond distances.



**Scheme 3.** Possible equilibrium in bistriazines **7**; nd: not detected.

In the second step the protonated species of isomers **I–VII** were studied as the hexafluorophosphates (Table S1) and perchlorates (Table S2).

Once again isomer **VI** was the most stable in the gas phase but in solution isomer **I** was the most stable both in CHCl<sub>3</sub> and DMSO, a finding that is consistent with the NMR spectra - from which an E configuration was predicted for the double bond [19]. The counterion (PF<sub>6</sub><sup>-</sup>) was located close to the diene and hydrogen bonds were formed between the fluorine and N–H atoms (Fig. 5).

For the perchlorate derivatives isomer **VI** was found to be more stable in the gas phase but in solution isomer **I** was the most stable in DMSO and isomer **V** in CHCl<sub>3</sub>. The counterion (ClO<sub>4</sub><sup>-</sup>) is again located close to the diene protons and hydrogen bonds are formed between an oxygen and the N–H atom (Fig. 6).

Introduction of substituents into the 1,5-diazapentadiene system was performed in a third step. The introduction of a chlorine atom into the diene did not lead to appreciable modifications. Once again, isomer **VI** is the most stable in the gas phase and isomer **I** in solution. However, the PF<sub>6</sub><sup>-</sup> anion is now located opposite to the chlorine atom (Fig. 7).

The introduction of the triazine rings into isomer **I**, which is the most stable in solution, leads to two rotamers with a small energy difference between them (Fig. 8).

In these two rotamers four hydrogen bonds are formed, two between the Cl and the N–H atoms and two more between the F and C–H atoms.

Finally, the amino groups were introduced into the triazine ring. The study was focused on the morpholino-substituted compound **7d** in order to reduce the number of isomers and, consequently, the computational cost. This advantage is due to the fact that rotation of the morpholino groups does not lead to different isomers and also because this compound was studied by NMR spectroscopy, in which splitting of the signals was observed. As described above, both rotamers have a very similar stability in solution (Fig. 9) and the results are therefore consistent with the <sup>1</sup>H-NMR data.

Bearing in mind the results of the computational calculations and the electronegativity of chlorine, we propose the formation of a hydrogen bond with the N<sup>+</sup>-H and a slow equilibrium between the isomers represented in Scheme 3. This proposal was supported by computational calculations. A signal for the N–H that participates in the hydrogen bond with the chlorine atom is not observed and, consequently, it is not coupled with H-2, which appears as a singlet.

**Table 8**  
Absorption maxima of bistriazines **7a–d** and comparison with the starting materials **5a–d** and **6**.

	CH <sub>2</sub> Cl <sub>2</sub>	CH <sub>3</sub> OH	DMF
	$\lambda_{\max}$ (nm) [log $\epsilon$ ]	$\lambda_{\max}$ (nm) [log $\epsilon$ ]	$\lambda_{\max}$ (nm) [log $\epsilon$ ]
<b>6</b>	327 [5.07]	321 [3.32]	324 [4.52]
<b>5a</b>	283 [4.60]	275 [3.76]	281 [4.85]
<b>7a</b>	277 [4.93], 380 [4.63]	278 [4.92], 382 [4.53]	281 [5.07], 387 [4.80]
<b>5b</b>	295 [4.67]	278 [4.59]	305 [4.28]
<b>7b</b>	306 [4.67], 377 [4.59]	301 [4.70], 383 [5.50]	308 [4.83], 384 [4.70]
<b>5c</b>	284 [4.97]	282 [4.70]	283 [4.60]
<b>7c</b>	283 [4.30], 378 [4.08]	282 [4.34], 372 [3.91]	280 [4.30], 388 [5.75]
<b>5d</b>	278 [4.27]	273 [4.21]	277 [4.45]
<b>7d</b>	285 [4.20], 383 [4.68]	285 [4.10], 382 [3.86]	386 [4.76]

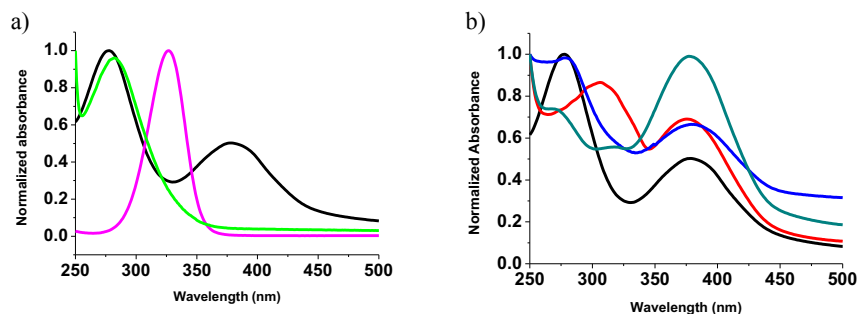


**Fig. 10.** a) Normalized absorption spectra of bistriazine **7a** (—) and comparison with the starting materials **5a** (—) and **6** (—). b) Normalized absorption spectra of bistriazines **7a** (—), **7b** (—), **7c** (—) and **7d** (—). Solvent  $\text{CH}_2\text{Cl}_2$ .

In contrast, the second N–H group is coupled with H-4 and the signal for this proton is a doublet.

## 2.6. Optoelectronic properties

### 2.6.1. Absorption properties

The absorption and emission spectra of the bistriazines were recorded in solvents with different polarities ( $\text{CH}_2\text{Cl}_2$ ,  $\text{CH}_3\text{OH}$  and DMF) at three different concentrations ( $10^{-5}$  M,  $10^{-6}$  M and  $10^{-7}$  M).

The use of  $\pi$ -conjugated molecules in photoluminescent materials was introduced by Tang and Van Slyke for OLED's [32] and today the preparation of organic compounds that are red, green, and especially blue emitters is one of the most active areas of research [33]. Other applications include the fabrication of optoelectronic devices such as solar cells sensitized with organic dyes (DSSC) or organic transistors.

The absorption maxima of bistriazines **7a-d** in the three solvents used are listed in Table 8 along with those of the starting materials **5a-d** and **6** in order to assess the influence of the spacer on the spectroscopic properties. Similarly, the normalized absorption spectra of **7a**, **5a**, and **6** are shown in Fig. 10.

Triazines **5a-d** give rise to a band at 278–308 nm in  $\text{CH}_2\text{Cl}_2$ . The position of this band depends on the nature of the substituent and it is bathochromically shifted in compounds that contain 1-naphthyl groups (**5b**, 294 nm) and hypsochromically shifted in those with morpholino groups (**5d**, 278 nm). A band due to the dienic system is observed at 327 nm for streptocyanine **6**.

The UV–vis spectra of bistriazines **7a-d** show two maxima at 279–308 and 378–380 nm. The band around 280 nm can be associated with  $n-\pi^*$  transition and the band around 380 nm are assigned to  $\pi-\pi^*$  transition of the conjugated backbone, due to their high absorption coefficients [9c]. This band is red shifted by 60–70 nm as a result of the higher conjugation with the phenyl groups. The relative intensities of both bands depend on the substitution of the triazine ring, with this effect being more intense in aryl-substituted bistriazines **7a-c** while the band at 380 nm is more intense in the morpholino derivative **7d** (Fig. 10b).

We have used theoretical models in order to reproduce the

**Table 9**

Wavelength (nm) of the vertical transitions the lowest excited-state for compound **7a**, calculated with various theoretical levels.

TD methodology	Abs (nm)
B3LYP/6-311 + G(d,p)//B3LYP/6-311 + G(d,p)	469.71
M062x/6-311 + G(d,p)//M062x/6-311 + G(d,p)	457.14
PBE(D3BJ)/6-311++G(2d,2p)//PBE(D3BJ)/6-311++G(2d,2p)	466.66
PBE(D3BJ)/6-311++G(2d,2p)//PBE0(D3BJ)/6-311++G(2d,2p)	469.32
B3LYP/6-311 + G(d,p)//CAM-B3LYP/6-311++G(2d,2p)	394.92

**Table 10**

Emission maxima of bistriazines **7a-d** and the starting materials **5a-d** and **6**.

	$\text{CH}_2\text{Cl}_2$	$\text{CH}_3\text{OH}$	DMF
	$\lambda_{\text{max}}$ (nm)	$\lambda_{\text{max}}$ (nm)	$\lambda_{\text{max}}$ (nm)
<b>6</b>	383	395	382
<b>5a</b>	409	399	298
<b>7a</b>	409, 432, 455	407, 430, 455	409, 435, 500
<b>5b</b>	379	378	379
<b>7b</b>	410, 435, 460	405, 430, 500	406, 431, 460
<b>5c</b>	380	359	374
<b>7c</b>	408, 433, 455	403, 428	455
<b>5d</b>	410	374	376
<b>7d</b>	408, 432, 454	404, 429, 455	410, 433, 455

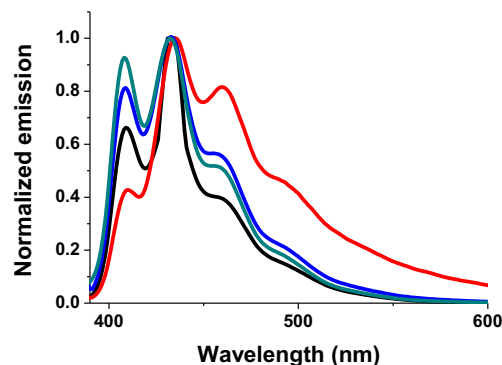


**Fig. 11.** Emission spectra of bistriazines **7a** (—), **7b** (—), **7c** (—) and **7d** (—). Solvent  $\text{CH}_2\text{Cl}_2$ . Excitation, see Table 11.

absorption spectra of these compounds. This methodology is a useful way to design new compounds with selected optoelectronic properties. For this purpose, TD-DFT (time-dependent density functional theory) is certainly the most popular method due to its remarkably small computational cost and to the availability of analytical derivatives allowing for easy exploration of the excited-state potential energy surface [34].

It was remarked the difficulty of setting up a theoretical protocol to reproduce the absorption spectrum of streptocyanine derivatives, probably due to the three possible limit configurations for the streptocyanine system [35]. Considering these difficulties we selected compound **7a**, with a reduced number of rotamers, for this study and we used different theory levels. The outcomes obtained are collected in Table 9.

The results indicate that the calculated absorption maxima are highly dependent on the level of calculation. In our case, most methods fail to accurately reproduce the experimental values and result in a large overestimation of the wavelength. However, for this

**Table 11**  
Emission maxima of bistriazines **7a–d** and the starting materials **5a–d** and **6** in CH<sub>2</sub>Cl<sub>2</sub>.

	$\lambda_{\max}$ (nm) [log $\epsilon$ ]	$\lambda_{\text{fluoresc}}$ (nm)	Stokes shift (cm <sup>-1</sup> )	$\lambda_{\text{excit}}$ (nm)	$\Phi_{\text{F}}$ (%)
<b>6</b>	327 [5.07]		4471	327	
<b>5a</b>	283 [4.60]	409	10886	280	
<b>7a</b>	277 [4.93], 380 [4.63]	409, 432, 455	9457, 3168	380	0.1
<b>5b</b>	295 [4.67]	379	7628	295	
<b>7b</b>	306 [4.67], 377 [4.59]	410, 435, 460	6152, 3467	381	0.4
<b>5c</b>	284 [4.97]	380	8895	284	
<b>7c</b>	283 [4.30], 378 [4.08]	408, 432, 455	10875, 3307	381	0.2
<b>5d</b>	278 [4.27]	410	9233	277	
<b>7d</b>	285 [4.20], 383 [4.68]	408, 432, 454	8421, 2962	385	0.2

type of compound, calculations at the B3LYP/6-311 + G(d,p)//CAM-B3LYP/6-311++G(2d,2p) level of theory gives an optimum correlation between experimental and theoretical results. On the study of excited states and transition between these, it is advisable to take precautions since the underestimation of charge-transfer (CT) excitation energies (especially in donor–acceptor systems) [36] is one of most common problem that exchange–correlation functionals suffer. This failure of the method is partly avoided using the Coulomb-attenuated CAM-B3LYP functional, leading to a correction that has been previously observed in the literature [37].

### 2.6.2. Emission properties

The emission maxima of bistriazines **7a–d** were recorded with irradiation at the two maxima in the absorption spectra and are collected in Table 10 for the three solvents used along with those of the starting materials **5a–d** and **6**. The emission spectra of **7a–d** are shown in Fig. 11 (a comparison with the starting materials is shown in Fig. S3).

Triazines **5** were poor emitters in solution and only compound **5d** showed a medium intensity fluorescence [14]. Similarly, bistriazines **7** showed only a low intensity emission in the fluorescence spectra, with the exception of **7a** in dichloromethane (Fig. S4). The strong intermolecular association produced in amino triazines can explain this result where hydrogen bonding and  $\pi$ -stacking produce fluorescence quenching. The highest fluorescence was usually observed on excitation of the band at 380 nm.

These bistriazines show emission over a wide range of wavelengths with a maximum at 432 nm and two other maxima at 408 and 455 nm. They show also a shoulder at 500 nm that can be ascribed to the formation of excimers [38], which are formed by the planar disposition of these compounds. This effect is especially important for compound **3b** with 1-naphthyl groups.

Very large Stokes shifts were observed, higher than 6000 cm<sup>-1</sup> (Table 11). These large values are typical in known systems and imply the formation of intermolecular excimers with a high degree

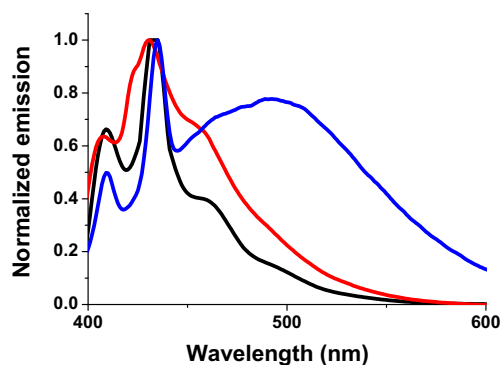


**Fig. 13.** Solvatochromism on the emission spectra of bistriazine **7a**. Excitation at 380 nm CH<sub>2</sub>Cl<sub>2</sub> (—), CH<sub>3</sub>OH (—) and DMF (—).

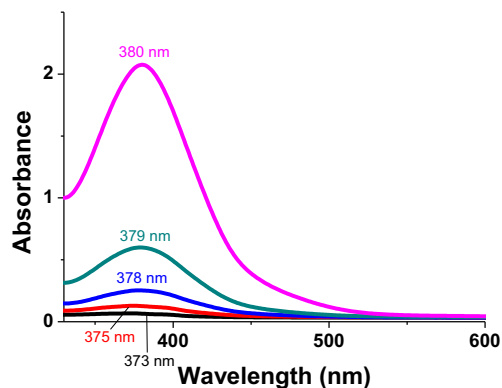


**Fig. 14.** Absorption spectra of bistriazine **7a** at different concentrations  $4.8 \times 10^{-7}$  M (—),  $7.2 \times 10^{-6}$  M (—),  $4.8 \times 10^{-6}$  M (—),  $2.4 \times 10^{-6}$  M (—) and  $4.8 \times 10^{-5}$  M (—).

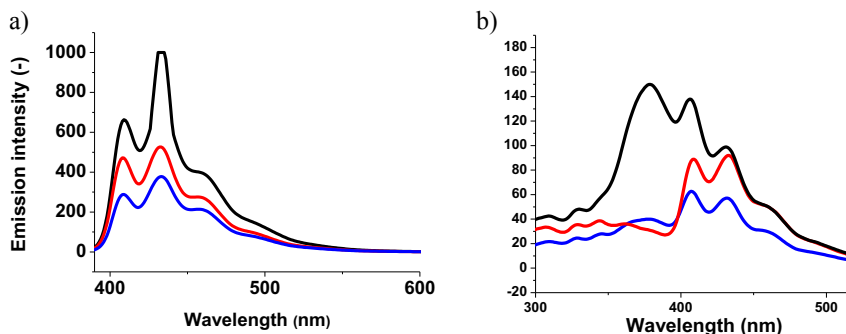


**Fig. 12.** Effect of concentration on the emission spectra of bistriazine **7a** in CH<sub>2</sub>Cl<sub>2</sub>  $2.4 \times 10^{-6}$  M (—),  $4.8 \times 10^{-6}$  M (—) and  $7.2 \times 10^{-6}$  M (—) a) Excitation at 380 nm b) Excitation at 280 nm.

of aggregation [39]. Excited state intramolecular charge transfer (ESIPT) have also been considered to explain the large Stokes shifts [40]. In our case, this possibility implies previous Z/E isomerization to adopt the conformation for the ESIPT or the participation of the Chlorine group, that has not been previously reported (Scheme S1).

Quantum yields were low but they are in the range of those described for cyanine dyes used for labelling of proteins that present of larger conjugation [41].

In streptocyanine **6**, triazines **5**, and bistriazines **7** the fluorescence intensity increased as the concentration decreased. This effect confirms again the formation of excimers that produce a quenching in the fluorescence at higher concentrations. The fluorescence increased at higher dilution, i.e., as a lower association was observed (Fig. 12). It is interesting to note that the on excitation at 280 nm the band at 380 nm disappears at higher concentrations.

### 2.6.3. Solvatochromism

In the absorption spectra solvent effects are negligible in the band at 280 nm whereas a small bathochromic shift in the band at 380 nm (maximum 9 nm) is observed in DMF and the intensity increases in this solvent (Fig. S2).

In the emission spectra of **7a**, the same pattern is observed in different solvents but a wide band at 500 nm was observed in DMF (Fig. 13). This band confirms again the formation of excimers [38] and is observed in all bistriazines especially in DMF but also in MeOH and CH<sub>2</sub>Cl<sub>2</sub> (Fig. S4).

### 2.6.4. Aggregation of bistriazines

Aggregation of bistriazines was qualitatively studied by recording the UV–vis spectra at various temperatures. The variation of the spectra with temperature is often considered to be more appropriate than concentration effects. This is because, with a single solution, it is possible to obtain a large number of data and to determine the transition from the monomeric to the completely assembled species and also to determine the mechanism of aggregation and even the thermodynamic parameters [37]. However, the effect observed was very small in the range of temperatures used in chloroform and the degree of aggregation is probably very high in these compounds. The low solubility of these compounds prevented the use of solvent with higher boiling point.

Therefore, the best results to differentiate these systems were obtained at different concentrations (Fig. 14).

An important point is that absorption depends on the concentration. Increasing the concentration does not produce a similar increase in the  $A_{\max}$  values and a small shift in the  $\lambda_{\max}$  is observed. In this situation, Lambert–Beer's law is not valid. This effect has been ascribed to an increase in the formation of aggregates that have the character of J aggregates with higher  $\lambda_{\max}$  and lower  $\epsilon_{\max}$  [42].

Considering the results described by Meijer et al. [43], we can tentatively propose an isodesmic mechanism for the self-association of bisimines **7**. In an isodesmic equilibrium every monomer addition to the growing chain is governed by a single equilibrium constant and there is a gradual increase in the number and length of the aggregated species. In this situation, Meijer deduced that it is only at high concentrations or for high association constants that long nanometer-sized objects are formed [43].

Numerous streptocyanines have been reported to form J-aggregates [44]. The aggregates in solution exhibit distinct changes in the absorption band as compared to the monomeric species. Various aggregation patterns of the dyes have been proposed from the spectral shifts. The bathochromically shifted J-bands (J for Jelly) and hypsochromically shifted H-bands (H for hypsochromic) of the aggregates have been explained in terms of molecular exciton coupling theory, i.e., coupling of transition moments of the

constituent dye molecules [45].

In our products, a strong association is produced and the monomeric species cannot be detected even in highly dilute solutions.

## 3. Conclusions

A new series of bistriazine substituted streptocyanines has been prepared by reaction of *p*-aminophenylaminotriazines **5** with 3-chloro-*N,N,N',N'*-tetramethyl-1,5-diaza-1,3-pentadienium hexafluorophosphate (**6**).

For the preparation of the starting triazines **5**, we have confirmed the differential sequential reactivity of the chloro-substituents in cyanuric chloride by determination of the Fukui constants. These results confirms that the increased substitution of the triazine ring results in a decrease in the electrophilic character of the triazine ring.

The structure of streptocyanines **7** was studied by computational calculations and NMR spectroscopy. These techniques provided evidence of an intramolecular hydrogen bond between the chlorine atom and the NH groups of the streptocyanine moiety that permits the differentiation of the two parts of the molecule.

The electronic spectra of streptocyanines **7** can be visualized, by comparison with the starting materials, as the sum of the two parts of the molecule, the triazine and the dienic structure. The streptocyanine part shows a large red shift because of the conjugation with the phenylene group. The new compounds show interesting optoelectronic properties; they are blue emitters, they show large Stokes shifts and a strong association in solution by formation of hydrogen bond and  $\pi$ -stacking that is reflected in an increase in the fluorescence intensity when the concentration is reduced.

## 4. Experimental

### 4.1. General

All the calculations included in this paper were performed using Gaussian 09 suite of programs [46].

All reagents and anhydrous solvents were purchased from commercial sources and used without further purification. 3-Chloro-*N,N,N',N'*-tetramethyl-1,5-diaza-1,3-pentadienium hexafluorophosphate (**6**) was prepared as previously described [47]. Reactions under microwave irradiation were performed in a CEM Discover monomode reactor with a dynamic method (temperature controlled). Temperature was measured with the IR pyrometer included in the microwave reactor. Melting points were determined in capillary tubes using a Büchi M-565 apparatus and are given corrected. IR spectra were obtained with a Thermo Nicolet-IR-100 spectrophotometer provided with ATR and a ZnSe lens. NMR spectra were recorded on Varian Inova 500 spectrometer with TMS as the internal standard. Assignment of the <sup>1</sup>H and <sup>13</sup>C signals was done with the aid of homo and heteronuclear 2D correlations (gCOSY y gHSQC) using the standard pulse sequences from Varian. The 2D exchange spectra (EXSY) were acquired in the phase-sensitive mode using the States-Haberhorn method [48]. Typically, a 3.1 kHz spectral width, 16 transients of 2048 data points were collected for each 400 t1 increments. A 1s relaxation delay, an 11s (908) pulse width and a 0.165s acquisition time were used. The free induction decays were processed with square cosine-bell filters in both dimensions and zero filling was applied prior to double Fourier transition. Determination of the kinetic parameters required two experiments with mixing times of 1 s (optimized) for the exchange experiment and 0.02 s for the non-exchange spectra, respectively. The cross peak/diagonal ratio was determined by integrating the volume under the peaks. Mass spectra were

recorded on a Bruker Autoflex II MALDI TOF/TOF spectrometer using DHB as the matrix. UV–vis spectra were recorded on a Varian Cary model 5000 UV–Vis–NIR spectrophotometer provided with control of temperature from –10 to 100 °C. Variable temperature experiments were recorded with  $1.038 \times 10^{-6}$  M solutions at 5-degree intervals and the temperature was stabilized for 5 min before recording the spectra. Fluorescence spectra were recorded on a Jasco FP-750 spectrophotometer. In both cases, standard quartz cells of 1 cm width were used. Spectra were recorded using solvents of spectroscopic grade in the conditions specified in Table 6. Determination of quantum yields were carried out on an Uvikon-XS spectrofluorimeter. Quantum yields for compounds **7** were determined experimentally using as standard a solution of quinine sulfate in Dichloromethane ( $\Phi_F = 0.54$ ) and applying the following equation [49].

$$\Phi_{Fsa} = \Phi_{Fst} * (A_{st}/A_{sa}) * (I_{sa}/I_{st}) * (n_{sa}/n_{st})^2$$

sa = sample; st = standard (quinine sulfate in  $\text{CH}_2\text{Cl}_2$ ); A = absorbance; I = integration of corrected fluorescence spectrum; n = refractive index of the solvent.

#### 4.2. Synthesis of 2-chloro-4,6-bis(aryl)amino-1,3,5-triazines **3a–c,d'**. General procedure

In a round-bottomed flask fitted with an addition funnel, cyanuric chloride (**1**) (1.84 g, 9.97 mmol) was dissolved in glacial acetic acid (30 mL). A solution of the appropriate amine (**2**) (24.94 mmol) and sodium acetate (2.566 g, 31.3 mmol) in acetic acid (10 mL) and water (10 mL) was added slowly with vigorous stirring. Efficient stirring was continued at room temperature for 12 h. The solid was filtered off and washed with hot water until the washing water gave a pH = 6 (ca. 400 mL) and the product was dried *in vacuo* in the presence of phosphorus pentoxide.

##### 4.2.1. 2-Chloro-4,6-bis(4'-methoxyphenylamino)-1,3,5-triazine (**3a**)

Following the general procedure for arylamines and using 4-methoxyaniline (**2a**) (93%). m.p. 199–200 °C (lit. 198–199 °C [23]).  $^1\text{H}$  NMR (DMSO- $d_6$ , 500 MHz, 353 K)  $\delta$  = 3.74 (s, 3H), 6.9 (br d, 2H), 7.5 (d,  $J$  = 8.8 Hz, 2H), 10.06 (bs, 2H).  $^{13}\text{C}$  NMR (DMSO- $d_6$ , 125 MHz, 353 K)  $\delta$  = 55.32, 114.57, 123.08, 130.16, 156.76, 164.29. IR:  $\nu_{\text{max}}$  = 3360, 2907, 2833, 1744, 1612, 1260, 988, 827  $\text{cm}^{-1}$ .

##### 4.2.2. 2-Chloro-4,6-bis(1-naphthylamino)-1,3,5-triazine (**3b**)

Following the general procedure for arylamines and using 1-naphthylamine (**2b**), stirring was continued for 48 h and acetic acid (150 mL) was added at 24 h (32%). m.p. 182–183 °C (from ethanol).  $^1\text{H}$  NMR (DMSO- $d_6$ , 500 MHz, 353 K)  $\delta$  = 7.35 (t,  $J$  = 7.9 Hz, 2H), 7.47 (m, 2H), 7.50 (ABCD system,  $J$  = 8.0, 8.0, 1.6 Hz, 4H), 7.75 (d,  $J$  = 7.9 Hz, 2H), 7.90 (ABCD system,  $J$  = 8.0, 1.6 Hz, 2H), 8.0 (ABCD system,  $J$  = 8.0, 1.6 Hz, 2H), 9.76 (bs, 2H).  $^{13}\text{C}$  NMR (DMSO- $d_6$ , 125 MHz, 353 K)  $\delta$  = 123.7, 124.0, 125.9, 126.6, 128.6, 129.7, 134.1, 134.5, 166.6, 169.6. IR:  $\nu_{\text{max}}$  = 3431, 3217, 3055, 1584, 1492, 785, 768  $\text{cm}^{-1}$ . MS (MALDI-TOF, DHB) calculated  $m/z$ , 397.1094, found, 397.809 [M + H] $^+$ .

##### 4.2.3. 2-Chloro-4,6-bis(diphenylamino)-1,3,5-triazine (**3c**)

In a round-bottomed flask fitted with a reflux condenser, a mixture of cyanuric chloride (**1**) (3.688 g, 20 mmol), diphenylamine (**2c**) (7.107 g, 42 mmol), DIPEA (8.1 mL) and di-*n*-butyl ether (20 mL) was heated under reflux (150 °C) for 6 h with efficient stirring. The mixture was poured into a mixture of ethanol (5 mL) and water (10 mL) in an ice bath and was crystallized at 4 °C for 12 h. The solid was filtered off in vacuum and washed with cold ethanol (100 mL

(61%). m.p. 216–220 °C (from ethanol) (Lit. 221–222 °C [50]).  $^1\text{H}$  NMR (DMSO- $d_6$ , 500 MHz)  $\delta$  = 7.08 (m, 12H), 7.16 (m, 8H).  $^{13}\text{C}$  NMR (DMSO- $d_6$ , 125 MHz)  $\delta$  = 126.1, 127.4, 128.7, 142.6, 165.6, 169.9. IR:  $\nu_{\text{max}}$  = 3647, 2980, 1738, 1200, 798, 752  $\text{cm}^{-1}$ . MS (MALDI-TOF, DHB) calculated  $m/z$ , 449.1407, found, 450.027 [M + H] $^+$ .

##### 4.2.4. 2,4-Dichloro-6-diphenylamino-1,3,5-triazine (**3c'**)

Following the general procedure for arylamines using diphenylamine (**2c**) (85%). m.p. 178–179 °C (from 2-propanol) (Lit. 172–174 [26]).  $^1\text{H}$  NMR (DMSO- $d_6$ , 500 MHz)  $\delta$  = 7.35 (m, 12H), 7.45 (m, 8H).  $^{13}\text{C}$  NMR (DMSO- $d_6$ , 125 MHz)  $\delta$  = 127.4, 127.7, 129.5, 141.8, 165.7, 169.1. MS (MALDI-TOF, DHB) calculated  $m/z$ , 316.0283, found, 316.892 [M + H] $^+$ .

##### 4.2.5. 2,4,6-Tris(diphenylamino)-1,3,5-triazine (**3c''**) [25]

In a round-bottomed flask fitted with a reflux condenser, a mixture of cyanuric chloride (**1**) (1.00 g, 5.4 mmol) and diphenylamine (**2c**) (4.86 g, 28.7 mmol) was heated under reflux (180–190 °C) with efficient stirring for 2 h. The crude mixture was cooled to 140 °C and poured into cold water (500 mL). The solid was filtered off in vacuum, extracted with acetone (3  $\times$  300 mL) and recrystallized (74%). m.p. 294–296 °C (from toluene) (Lit. 297–298 °C [25]).  $^1\text{H}$  NMR (DMSO- $d_6$ , 500 MHz)  $\delta$  = 7.50 (br, 15H), 7.92 (br, 10H).  $^{13}\text{C}$  NMR (DMSO- $d_6$ , 125 MHz)  $\delta$  = 123.5, 126.5, 128.4, 134.1, 166.2. MS (MALDI-TOF, DHB) calculated 582.2532, found,  $m/z$  583.361 [M + H] $^+$ .

##### 4.2.6. 2-Chloro-4,6-bis(morpholino)-1,3,5-triazine (**3d**)

In a round-bottomed flask fitted with an addition funnel, cyanuric chloride (**1**) (2.160 g, 11.7 mmol) was dissolved in acetone (20 mL) and cooled in an ice bath. A solution of morpholine (**2d**) (2.3 mL, 25.8 mmol) and DIPEA (4.6 mL) in acetone (15 mL) was added slowly keeping the temperature at 4–5 °C and stirring was continued for 3 h in the ice bath and for 24 h at room temperature. The solid was filtered off, washed with acetone (3  $\times$  10 mL) and the solvent was removed in vacuum to give an oily residue, which was dissolved in hot ethanol (100 mL) and crystallized on cooling (71%). m.p. 158–159 °C (Lit. 173 °C [51]).  $^1\text{H}$  NMR (DMSO- $d_6$ , 500 MHz)  $\delta$  = 3.61 (bs, 8H), 3.69 (bs, 8H).  $^{13}\text{C}$  NMR (DMSO- $d_6$ , 125 MHz)  $\delta$  = 43.5, 66, 164.8, 168.7. IR:  $\nu_{\text{max}}$  = 3024, 2943, 1738, 1217, 791  $\text{cm}^{-1}$ .

#### 4.3. Synthesis of 2-(4-aminophenylamino)-4,6-bis(alkyl or arylamino)-1,3,5-triazines (**5**). General procedure [14]

*p*-Phenylenediamine and the appropriate chlorotriazine **3** (0.3 mmol), and diisopropylethylamine (DIPEA) in a 3:1:1 ratio were dissolved in anhydrous DMSO (1 mL). The mixture was introduced into a microwave flask fitted with a reflux condenser and a silica gel tube under argon. The mixture was irradiated under microwaves for 10 min at 70 W and 140 °C. Water (10 mL) was added to the crude mixture, submitted to ultrasounds for 15 min and filtered to give the pure product.

##### 4.3.1. 2-(4-Aminophenylamino)-4,6-bis(4-methoxyphenylamino)-1,3,5-triazine (**5a**)

Following the general procedure using compound **3a** (98%). m.p. 87–89 °C (Lit. 85–89 °C [50]).  $^1\text{H}$  NMR (DMSO- $d_6$ , 500 MHz)  $\delta$  = 3.73 (s, 6H), 4.80 (bs, 2H), 6.50 (d,  $J$  = 8.8 Hz, 2H), 6.80 (d,  $J$  = 8.8 Hz, 4H), 7.32 (bs, 2H), 7.70 (bs, 4H), 8.80 (bs, 1H), 8.95 (bs, 2H). IR:  $\nu_{\text{max}}$  = 3734, 2999, 1734, 1614, 1217, 791, 731  $\text{cm}^{-1}$ . UV:  $\lambda_{\text{max}}$  ( $\text{CH}_2\text{Cl}_2$ ) 282 nm ( $\epsilon$  60000  $\text{dm}^3 \text{mol}^{-1} \text{cm}^{-1}$ ).

#### 4.3.2. 2-(4-Aminophenylamino)-4,6-bis(1-naphthylamino)-1,3,5-triazine (**5b**)

Following the general procedure using compound **3b** (98%), m.p. 103–106 °C (decomp.). <sup>1</sup>H NMR (DMSO-*d*<sub>6</sub>, 500 MHz)  $\delta$  = 4.60 (s, 2 H), 6.25 (d, *J* = 8.8 Hz, 2H), 7.09 (d, *J* = 8.8 Hz), 7.43 (t, *J* = 8.1 Hz), 7.50 (ABCD system, *J* = 8.0, 8.0, 1.6 Hz), 7.60 (d, *J* = 7.3 Hz, 2H), 7.72 (d, *J* = 8.2, 2H), 7.91 (ABCD system, *J* = 8.0, 1.6 Hz, 2H), 8.02 (ABCD system, *J* = 8.0, 1.6 Hz, 2H), 8.55 (bs, 1H), 8.97 (bs, 2H). <sup>13</sup>C NMR (DMSO-*d*<sub>6</sub>, 125 MHz)  $\delta$  = 113.0, 121.1, 123, 124.4, 125.1, 125.3, 127.4, 128.7, 128.9, 133.3, 134.5, 143, 163.6, 165.5. IR:  $\nu_{\max}$  = 3395, 3046, 2980, 1738, 1587, 1479, 806, 791, 770 cm<sup>-1</sup>. UV:  $\lambda_{\max}$  (CH<sub>2</sub>Cl<sub>2</sub>) 294 nm ( $\epsilon$  dm<sup>3</sup> mol<sup>-1</sup> 110000). MS: (MALDI-TOF, DHB) calculated *m/z*, 469.2015, found, 470.081 [M + H]<sup>+</sup>. Found: C, 74.47; H, 4.75; N, 21.12. C<sub>29</sub>H<sub>23</sub>N<sub>7</sub> requires C, 74.18; H, 4.94; N, 20.88%.

#### 4.3.3. 2-(4-Aminophenylamino)-4,6-bis(diphenylamino)-1,3,5-triazine (**5c**)

Following the general procedure using compound **3c** (99%), m.p. 162–164 °C (decomp.). <sup>1</sup>H NMR (DMSO-*d*<sub>6</sub>, 500 MHz)  $\delta$  = 4.59 (s, 2 H), 6.17 (d, *J* = 8.8 Hz, 2H), 7.00 (d, *J* = 8.8 Hz, 2H), 7.14 (m, 2H), 7.22 (m, 4H), 7.29 (m, 4H), 8.72 (s, H). <sup>13</sup>C NMR (DMSO-*d*<sub>6</sub>, 125 MHz)  $\delta$  = 113.2, 120.3, 124.6, 127.2, 127.9, 129.1, 142.7, 143.4, 163, 165.3. IR:  $\nu_{\max}$  = 3373, 3024, 2968, 1737, 802, 754, 689 cm<sup>-1</sup>. UV:  $\lambda_{\max}$  (CH<sub>2</sub>Cl<sub>2</sub>) 283 nm ( $\epsilon$ /dm<sup>3</sup> mol. cm<sup>-1</sup> 120000). MS: (MALDI-TOF, DHB) calculated *m/z*, 521.6280, found, 522.372 [M + H]<sup>+</sup>. Found: C, 76.28; H, 4.98; N, 18.62. C<sub>33</sub>H<sub>27</sub>N<sub>7</sub> requires C, 75.99; H, 5.22; N, 18.80%.

#### 4.3.4. 2-(4-Aminophenylamino)-4,6-bis(morpholino)-1,3,5-triazine (**5d**)

Following the general procedure using compound **3d**. Microwave irradiation (130 °C, 90 W) for 90 min (94%). m.p. 208–210 °C (decomp.). <sup>1</sup>H NMR (DMSO-*d*<sub>6</sub>, 500 MHz)  $\delta$  = 3.58 (m, 8H), 3.63 (m, 8H), 4.70 (s, 2H), 6.50 (d, *J* = 8 Hz, 2H), 7.2 (d, *J* = 8 Hz, 2H), 8.59 (s, 1H). <sup>13</sup>C NMR (DMSO-*d*<sub>6</sub>, 125 MHz)  $\delta$  = 43.7, 66.5, 114.2, 122.3, 129.7, 144.1, 164.4, 165.2. IR:  $\nu_{\max}$  = 3744, 2968, 1738, 1364, 1217, 802 cm<sup>-1</sup>. UV:  $\lambda_{\max}$  (CH<sub>2</sub>Cl<sub>2</sub>) 275 nm ( $\epsilon$ /dm<sup>3</sup> mol. cm<sup>-1</sup> 50000). MS: (MALDI-TOF, DHB) calculated *m/z*, 357.1913, found, 358.005 [M + H]<sup>+</sup>. Found: C, 56.90; H, 6.61; N, 27.30. C<sub>17</sub>H<sub>23</sub>N<sub>7</sub>O<sub>2</sub> requires C, 57.13; H, 6.49; N, 27.43%.

#### 4.4. Synthesis of streptocyanines (**7**). General procedure [47]

In a round-bottomed flask fitted with a reflux condenser, a mixture of compounds **5** (0.378 mmol) and **6** (0.058 g, 0.189 mmol) in dry ethanol (25 mL) was heated under reflux for 4 h. The solvent was removed in vacuum to give the pure product after recrystallization from 2-propanol.

#### 4.4.1. 1,5-{N,N'-bis-4-[(4,6-bis(4'-methoxyphenylamino)-1,3,5-triazin-2-yl)-aminophenyl]-3-chloro-1,5-diaza-1,3-pentanodienium hexafluorophosphate (**7a**)

Following the general procedure using compound **5a**, (20%), m.p. 185–187 °C (decomp.) (orange powder). <sup>1</sup>H NMR (DMSO-*d*<sub>6</sub>, 500 MHz)  $\delta$  = 3.75 (s, 12H), 6.88 (d, *J* = 8.8 Hz, 8H), 7.26 (bs, 4H), 7.64 (bs, 8H), 7.83 (bs, 8H), 8.24 (bs, 2H), 8.99 (bs, 4H), 9.09 (bs, 2H). <sup>13</sup>C NMR (DMSO-*d*<sub>6</sub>, 125 MHz)  $\delta$  = 55.2, 94.3, 113.5, 120.8, 122.1, 132, 140.2, 154.6, 163.9, 164. IR:  $\nu_{\max}$  = 3647, 2986, 1748, 1734, 1624, 1254, 1105, 837 cm<sup>-1</sup>. UV:  $\lambda_{\max}$  (CH<sub>2</sub>Cl<sub>2</sub>) 278, 375 nm ( $\epsilon$ /dm<sup>3</sup> mol. cm<sup>-1</sup> 90000, 50000). MS: (MALDI-TOF, DHB) calculated *m/z*, 929.3515, found, 929.367 [M + H]<sup>+</sup>. Found: C, 54.68; H, 4.39; N, 18.30. C<sub>49</sub>H<sub>46</sub>ClF<sub>6</sub>N<sub>14</sub>O<sub>4</sub>P requires C, 54.73; H, 4.31; N, 18.23%.

#### 4.4.2. 1,5-{N,N'-bis-4-[4,6-bis(1-naphthylamino)-1,3,5-triazin-2-yl)-aminophenyl]-3-chloro-1,5-diaza-1,3-pentanodienium hexafluorophosphate (**7b**)

Following the general procedure using compound **5b**, (48%), m.p. 148–151 °C (decomp.) (orange powder). <sup>1</sup>H NMR (DMSO-*d*<sub>6</sub>, 500 MHz)  $\delta$  = 6.88 (bs, 4H), 7.20 (bs, 2H), 7.45 (m, 8H), 7.52 (ABCD system, *J* = 8.0, 8.0, 1.6 Hz, 8 H), 7.60 (d, *J* = 7.2 Hz, 4H), 7.75 (d, *J* = 8.1 Hz, 4H), 7.95 (ABCD system, *J* = 8.0, 1.6 Hz, 4H), 8.05 (ABCD system, *J* = 8.0, 1.6 Hz, 4H), 8.99 (bs, 2H), 9.13 (bs, 4H). <sup>13</sup>C NMR (DMSO-*d*<sub>6</sub>, 125 MHz)  $\delta$  = 98, 120.3, 123.5, 123.7, 125.1, 125.5, 125.6, 125.8, 127.9, 129.5, 133.8, 134.8, 164.1, 166. IR:  $\nu_{\max}$  = 3647, 2988, 1748, 1607, 839, 770 cm<sup>-1</sup>. UV:  $\lambda_{\max}$  (CH<sub>2</sub>Cl<sub>2</sub>) 304, 373 nm ( $\epsilon$ /dm<sup>3</sup> mol. cm<sup>-1</sup> 60000, 50000). MS: (MALDI-TOF, DHB) calculated *m/z*, 1009.3718, found, 1009.419 [M + H]<sup>+</sup>. Found: C, 63.50; H, 4.10; N, 16.85. C<sub>61</sub>H<sub>46</sub>ClF<sub>6</sub>N<sub>14</sub>P requires C, 63.40; H, 4.01; N, 16.97%.

#### 4.4.3. 1,5-{N,N'-bis-4-[4,6-bis(diphenylamino)-1,3,5-triazin-2-yl)-aminophenyl]-3-chloro-1,5-diaza-1,3-pentanodienium hexafluorophosphate (**7c**)

Following the general procedure using compound **5c**, (44%), m.p. 245–248 °C (decomp.) (orange powder). <sup>1</sup>H NMR (DMSO-*d*<sub>6</sub>, 500 MHz, 80 °C)  $\delta$  = 6.81 (bs, 2H), 6.85 (d, *J* = 9.1 Hz, 4H), 7.18 (d, *J* = 7.0 Hz, 8H), 7.2–7.4 (m, 32H), 7.31 (m, 4H), 8.17 (bs, 2H), 9.1 (bs, 2H). <sup>13</sup>C NMR (DMSO-*d*<sub>6</sub>, 125 MHz, 80 °C)  $\delta$  = 98.1, 116.6, 119.9, 125.5, 127.8, 128.6, 129.1, 143.3, 157, 161.6, 163.3.  $\nu_{\max}$  = 3669, 3647, 3379, 1734, 1647, 1400, 837, 746, 696 cm<sup>-1</sup>. UV:  $\lambda_{\max}$  (CH<sub>2</sub>Cl<sub>2</sub>) 279, 381 nm ( $\epsilon$ /dm<sup>3</sup> mol. cm<sup>-1</sup> 30000, 20000). MS: (MALDI-TOF, DHB) calculated *m/z*, 1113.4344, found, 1113.458 [M + H]<sup>+</sup>. Found: C, 65.70; H, 4.39; N, 15.65. C<sub>69</sub>H<sub>54</sub>ClF<sub>6</sub>N<sub>14</sub>P requires C, 65.79; H, 4.32; N, 15.57%.

#### 4.4.4. 1,5-{N,N'-bis-4-[4,6-bis(N,N'-morpholino)-1,3,5-triazin-2-yl)-aminophenyl]-3-chloro-1,5-diaza-1,3-pentanodienium hexafluorophosphate (**7d**)

Following the general procedure using compound **5d**, (29%), m.p. 234–237 °C (decomp.) (yellow powder). <sup>1</sup>H NMR (DMSO-*d*<sub>6</sub>, 500 MHz, 80 °C)  $\delta$  = 3.62 (m, 16H), 3.71 (m, 16H), 7.13 (d, *J* = 8.8 Hz, 2H), 7.60 (d, *J* = 8.8 Hz, 2H), 8.09 (bs, 2H), 8.70 (bs, 2H). <sup>13</sup>C NMR (DMSO-*d*<sub>6</sub>, 125 MHz, 80 °C)  $\delta$  = 42.9, 66.5, 106.1, 115.5, 120.2, 163.6, 164.5. IR:  $\nu_{\max}$  = 3647, 2980, 1748, 1734, 1558, 1217, 1030, 825 cm<sup>-1</sup>. UV:  $\lambda_{\max}$  (CH<sub>2</sub>Cl<sub>2</sub>) 377 nm ( $\epsilon$ /dm<sup>3</sup> mol. cm<sup>-1</sup> 40000). MS: (MALDI-TOF, DHB) calculated *m/z*, 785.3515, found, 785.185 [M + H]<sup>+</sup>. Found: C, 47.78; H, 4.91; N, 21.15. C<sub>37</sub>H<sub>46</sub>ClF<sub>6</sub>N<sub>14</sub>O<sub>4</sub>P requires C, 47.72; H, 4.98; N, 21.06%.

#### Acknowledgements

Financial support from the Spanish Ministerio de Ciencia e Innovación CTQ2011-22410, CTQ2014-54987-P and PEII-2014-002A is gratefully acknowledged. F.L. acknowledges a predoctoral grant from the Programa de Apoyos para la Superación del Personal Académico (PASPA) of the UNAM. We acknowledge M.A. Herrero for recording the MALDI-TOF spectra and technical support from the High Performance Computing Service of the Universidad de Castilla-La Mancha.

#### Appendix A. Supplementary data

Supplementary data related to this article can be found at <http://dx.doi.org/10.1016/j.dyepig.2016.04.016>.

#### References

- [1] Meier H. Conjugated oligomers with terminal donor–acceptor substitution. *Angew Chem Int Ed* 2005;44:2482–506. <http://dx.doi.org/10.1002/>

- anie.200461146.
- [2] Schenning APHJ, Meijer EW. Supramolecular electronics; nanowires from self-assembled  $\pi$ -conjugated systems. *Chem Commun* 2005;3245–58. <http://dx.doi.org/10.1039/b501804h>.
- [3] Mulliken RS, Person WB. Donor-acceptor complexes. *Annu Rev Phys Chem* 1962;13:107–26. <http://dx.doi.org/10.1146/annurev.pc.13.100162.000543>.
- [4] (a) Foster R. Organic charge-transfer complexes. New York: Academic Press; 1969.  
 (b) Foster R. Electron donor-acceptor complexes. *J Phys Chem* 1980;84:2135–41. <http://dx.doi.org/10.1021/j100454a006>.  
 (c) Espildora E, Delgado JL, Martín N. Donor-acceptor hybrids for organic electronics. *Isr J Chem* 2013;54:429–39. <http://dx.doi.org/10.1002/ijch.201400007>.
- [5] (a) Liu J, Wang K, Xu F, Tang Z, Zheng W, Zhang J, et al. Synthesis and photovoltaic performances of donor- $\pi$ -acceptor dyes utilizing 1,3,5-triazine as  $\pi$  spacers. *Tetrahedron Lett* 2011;52:6492–6. <http://dx.doi.org/10.1016/j.tetlet.2011.09.116>.  
 (b) Cai Z, Zhou M, Li B, Chen Y, Jin F, Huang J. Investigation of photophysical properties of new branched compounds with triazine and benzimidazole units. *New J Chem* 2014;38:3042–9. <http://dx.doi.org/10.1039/C4NJ00360H>.  
 (c) Jiang Y, Wang Y, Hua J, Tang J, Li B, Qian S, et al. Multibranching triarylamine end-capped triazines with aggregation induced emission and large two-photon absorption cross-sections. *Chem Commun* 2010;46:4689–91. <http://dx.doi.org/10.1039/C0CC00803F>.  
 (d) Zou L, Liu Z, Yan X, Liu Y, Fu Y, Liu J, et al. Star-shaped d- $\pi$ -a molecules containing a 2,4,6-tri(thiophen-2-yl)-1,3,5-triazine unit: synthesis and two-photon absorption properties. *Eur J Org Chem* 2009;5587–93. <http://dx.doi.org/10.1002/ejoc.200900641>.  
 (e) Gong X, Zhou Z, Zhang S, Zhuo S, Huang X, Jiang S, et al. A novel nitrogen-containing compound with d- $\pi$ -a structure: theoretical and experimental study. *Can J Chem* 2014;92:411–6. <http://dx.doi.org/10.1139/cjc-2013-0437>.  
 (f) Yan Yongli, Zhao Yong Sheng. Organic nanophotonics: from controllable assembly of functional molecules to low-dimensional materials with desired photonic properties. *Chem Soc Rev* 2014;43:4325–40. <http://dx.doi.org/10.1039/C4CS00098F>.
- [6] Padalcar VS, Patil VS, Sekar N. Synthesis and photo-physical properties of fluorescent 1,3,5-triazine styryl derivatives. *Chem Cent J* 2011;5:77. <http://dx.doi.org/10.1039/C4CS00098F>. DOI:10.1186/1752-153X-5-77.
- [7] Do K, Choi H, Lim K, Jo H, Cho JW, Nazeeruddin MK, et al. Star-shaped hole transporting materials with a triazine unit for efficient perovskite solar cells. *Chem Commun* 2014;50:10971–4. <http://dx.doi.org/10.1039/C4CC04550>.
- [8] (a) Quesada M, de la Pena-O'Shea VA, Aromi G, Geremia S, Massera C, Roubeau O, et al. A Molecule-based nanoporous material showing tuneable spin-crossover behavior near room temperature. *Adv Mater* 2007;19:1397–402. <http://dx.doi.org/10.1002/adma.200602284>.  
 (b) Yuste C, Cañadillas-Delgado L, Labrador A, Delgado FS, Ruiz-Pérez C, Lloret F, et al. Low-dimensional copper(II) complexes with the trinucleating ligand 2,4,6-tris(di-2-pyridylamine)-1,3,5-triazine: synthesis, crystal structures, and magnetic properties. *Inorg Chem* 2009;48:6630–40. <http://dx.doi.org/10.1021/jc900599g>.
- [9] (a) Kulkarni AP, Tonzola CJ, Babel A, Jenekhe SA. Electron transport materials for organic light-emitting diodes. *Chem Mater* 2004;16:4556–73. <http://dx.doi.org/10.1021/cm049473>.  
 (b) Rothmann MM, Haneder S, Da Como E, Lennartz C, Schildknecht C, Strohmriegel P. Donor-substituted 1,3,5-triazines as host materials for blue phosphorescent organic light-emitting diodes. *Chem Mater* 2010;22:2403–10. <http://dx.doi.org/10.1021/cm9033879>.  
 (c) An ZF, Chen RF, Yin J, Xie GH, Shi HF, Tsuboi T, et al. Conjugated asymmetric donor-substituted 1,3,5-triazines: new host materials for blue phosphorescent organic light-emitting diodes. *Chem Eur J* 2011;17:10871–8. <http://dx.doi.org/10.1002/chem.201101118>.  
 (d) Inomata H, Goushi K, Masuko T, Konno T, Imai T, Sasabe H, et al. High-efficiency organic electrophosphorescent diodes using 1,3,5-triazine electron transport materials. *Chem. Mater* 2004;16:1285–91. <http://dx.doi.org/10.1021/cm034689>.  
 (e) Pang J, Tao Y, Freiberg S, Yang XP, D'lorio M, Wang S. Syntheses, structures, and electroluminescence of new blue luminescent star-shaped compounds based on 1,3,5-triazine and 1,3,5-trisubstituted benzene. *J Mater Chem* 2002;12:206–12. <http://dx.doi.org/10.1039/B105422H>.  
 (f) Liu J, Teng MY, Zhang XP, Wang K, Li CH, Zheng YX, et al. Efficient blue emitters based on 1,3,5-triazine for nondoped organic light emitting diode applications. *Org Electron* 2012;13:2177–84. <http://dx.doi.org/10.1016/j.orgel.2012.06.013>.  
 (g) Volz D, Wallesch M, Fléchon C, Danz M, Verma A, Navarro JM, et al. From iridium and platinum to copper and carbon: new avenues for more sustainability in organic light-emitting diodes. *Green Chem* 2015;17:1988–2011. <http://dx.doi.org/10.1039/C4GC02195A>.
- [10] (a) Zheng Z, Zhou HP, Xu GY, Yu ZP, Yang XF, Cheng LH, et al. Properties of multi-branched styryl derivatives containing p-bond and s-electron pair as bridge based on 1,3,5-triazine. *Tetrahedron* 2012;68:6569–74. <http://dx.doi.org/10.1016/j.tet.2012.05.050>.  
 (b) Meng F, Li B, Shixiong Q, Chem K, Tian H. Enhanced two-photon properties of tri-branched styryl derivatives based on 1,3,5-triazine. *Chem Lett* 2004;33:470–1. <http://dx.doi.org/10.1246/cl.2004.470>.
- [11] Kawamura K, Schmitt J, Barnett M, Salmi H, Ley C, Allonas X. Squarylium-triazine dyad as a highly sensitive photoradical generator for red light. *Chem Eur J* 2013;19:12853–8. <http://dx.doi.org/10.1002/chem.201300622>.
- [12] Wu Y, Zhu W. Organic Sensitizers from d- $\pi$ -a to d-a- $\pi$ -a: effect of the internal electron-withdrawing units on molecular absorption, energy levels and photovoltaic performances. *Chem Soc Rev* 2013;42:2039–58. <http://dx.doi.org/10.1039/c2cs35346f>.
- [13] (a) Wan M, Zhou S, Jiao P, Cao C, Guo J. Synthesis, physical properties and cytotoxicity of stilbene-triazine derivatives containing amino acid groups as fluorescent whitening agents. *J Fluoresc* 2013;23:1099–105. <http://dx.doi.org/10.1007/s10895-013-1239-1>.  
 (b) Rodrigues AD, Imberdis T, Perrier V, Robitzer M. Improved synthesis of a quaterthiophene-triazine-diamine derivative, a promising molecule to study pathogenic prion proteins. *Tetrahedron Lett* 2015;56:368–73. <http://dx.doi.org/10.1016/j.tetlet.2014.11.098>.  
 (c) Geist MF, Chartrand D, Cibian M, Zieschang F, Hanan GS, Kurth DG. A facile route to bis(pyridyl-1,3,5-triazine) ligands with fluorescing properties. *Eur J Org Chem* 2015;2366–73. <http://dx.doi.org/10.1002/ejoc.201403521>.
- [14] Ruiz-Carretero A, Noguez O, Herrera T, Ramírez JR, Sánchez-Migallón A, de la Hoz A. Microwave-assisted selective synthesis of mono- and bistriazines with  $\pi$ -conjugated spacers and study of the optoelectronic properties. *J Org Chem* 2014;79:4909–19. <http://dx.doi.org/10.1021/jo500480r>.
- [15] Mishra A, Behera RK, Behera PK, Mishra BK, Behera GB. Cyanines during the 1990's: a review. *Chem Rev* 2000;100:1973–2011. <http://dx.doi.org/10.1021/cr990402t>.
- [16] (a) Mishra A, Fischer MKR, Buerle P. Metal-free organic dyes for dye-sensitized solar cells: from structure: property relationships to design rules. *Angew Chem Int Ed* 2009;48:2474–99. <http://dx.doi.org/10.1002/anie.200804709>.  
 (b) Hagfeldt A, Boschloo G, Sun L, Kloo L, Pettersson H. Dye-sensitized solar cells. *Chem Rev* 2010;110:6595–663. <http://dx.doi.org/10.1021/cr900356p>, and references therein.
- [17] (a) Véron AC, Zhang H, Linden A, Nüesch F, Heier J, Hany R, et al. NIR-absorbing heptamethine dyes with tailor-made counterions for application in light to energy conversion. *Org Lett* 2014;16:1044–7. <http://dx.doi.org/10.1021/ol4034385>.  
 (b) Bricks JL, Kachkovskii AD, Slominskii YL, Gerasov AO, Popov SV. Molecular design of near infrared polymethine dyes: a review. *Dyes Pigments* 2015;121:238–55. <http://dx.doi.org/10.1016/j.dyepig.2015.05.016>.  
 (c) Henary M, Levitz A. Synthesis and applications of unsymmetrical carbocyanine dyes. *Dyes Pigments* 2013;99:1107–16. <http://dx.doi.org/10.1016/j.dyepig.2013.08.001>.  
 (d) Guo Z, Park S, Yoon J, Shin I. Recent progress in the development of near-infrared fluorescent probes for bioimaging applications. *Chem Soc Rev* 2014;43:16–29. <http://dx.doi.org/10.1039/c3cs60271k>.
- [18] Cuthbertson WW, Moffatt JS. Contributions to the chemistry of synthetic antimetabolites. part VI. some derivatives of 1,3,5-triazine. *J Chem Soc* 1948:561–4. <http://dx.doi.org/10.1039/JR9480000561>.
- [19] (a) Bultinck P, Carbó-Dorca R, Langenaecker W. Negative Fukui functions: new insights based on electronegativity equalization. *J Chem Phys* 2003;118:4349–56. <http://dx.doi.org/10.1063/1.1542875>.  
 (b) Melin J, Ayers PW, Ortiz JV. Removing electrons can increase the electron density: a computational study of negative Fukui functions. *J Phys Chem A* 2007;111:10017–9. <http://dx.doi.org/10.1021/jp075573d>.  
 (c) Bultinck P, Carbó-Dorca R. Negative and infinite Fukui functions: the role of diagonal dominance in the hardness matrix. *J Mater Chem* 2003;13:67–74.  
 (d) Yang W, Mortier WJ. The use of global and local molecular parameters for the analysis of the gas-phase basicity of amines. *J Am Chem Soc* 1986;108:5708–11. <http://dx.doi.org/10.1021/ja00279a008>.
- [20] (a) Kohn W, Becke AD, Parr RG. Density functional theory of electronic structure. *J Phys Chem* 1996;100:12974–80. <http://dx.doi.org/10.1021/jp960669l>.  
 (b) Becke AD. Density-functional thermochemistry. iii. the role of exact exchange. *J Chem Soc* 1993;98:5648–52. <http://dx.doi.org/10.1063/1.464913>.  
 (c) Becke AD. Density-functional exchange-energy approximation with correct asymptotic behaviour. *Phys Rev A* 1988;38:3098–100. <http://dx.doi.org/10.1103/PhysRevA.38.3098>.
- [21] Parr RG, Yang W. In density-functional theory of atoms and molecules. New York: Oxford University Press; 1994.
- [22] (a) Ditchfield R, Hehre WJ, Pople JA. Self-consistent molecular-orbital methods. IX. an extended gaussian-type basis for molecular-orbital studies of organic molecules. *J Chem Phys* 1971;54:724–8. <http://dx.doi.org/10.1063/1.1674902>.  
 (b) Hehre WJ, Ditchfield R, Pople JA. Self-consistent molecular orbital methods. XII. Further extensions of Gaussian-Type basis sets for use in molecular orbital studies of organic molecules. *J Chem Phys* 1972;56:2257–61. <http://dx.doi.org/10.1063/1.1677527>.
- [23] Kolmakov KA. An efficient, "green" approach to aryl amination of cyanuric chloride using acetic acid as solvent. *J Heterocycl Chem* 2008;45:533–9. <http://dx.doi.org/10.1002/jhet.5570450236>.
- [24] Gonçalves MST. Fluorescent labeling of biomolecules with organic probes. *Chem Rev* 2009;109:190–212. <http://dx.doi.org/10.1021/cr0783840>.
- [25] Selby TD, Stickley KR, Blackstock SC. Triamino-s-triazine triradical trications. an experimental study of triazine as a magnetic coupling unit. *Org Lett* 2000;2:171–4. <http://dx.doi.org/10.1021/ol9912736>.
- [26] Thurston JT, Dudley JR, Kaiser DW, Hechenbleikner I, Schaefer FC, Holm-Hansen D. Cyanuric chloride derivatives. I. aminochloro-s-triazines. *J Am*

- Chem Soc 1951;73:2981–3. <http://dx.doi.org/10.1021/ja01151a001>.
- [27] (a) Elguero J, Díaz-Ortiz A, Moreno A, de la Hoz A, Martínez LJ, Sánchez-Migallón A. Solvent-free preparation of tris-pyrazolyl-1,3,5-triazines. *Tetrahedron* 2001;57:4397–403. [http://dx.doi.org/10.1016/S0040-4020\(01\)00340-4](http://dx.doi.org/10.1016/S0040-4020(01)00340-4).  
(b) Díaz-Ortiz A, Elguero J, Foces-Foces C, de la Hoz A, Moreno A, Moreno S, et al. Synthesis, structural determination and dynamic behavior of 2-chloro-4,6-bis(pyrazolylamino)-1,3,5-triazines. *Org Biomol Chem* 2003;1:4451–7. <http://dx.doi.org/10.1039/B310693D>.  
(c) Ghiviriga I, Oniciu DC. Steric hindrance to the solvation of melamines and consequences for non-covalent synthesis. *Chem Commun* 2002:2718–9. <http://dx.doi.org/10.1039/B206811G>.  
(d) Moral M, Ruiz-Carretero A, Díaz-Ortiz A, López I, Sánchez-Migallón A, de la Hoz A. Solvent-free microwave-assisted synthesis of new 2,4-dimethoxybenzylaminotriazines. *Arkivoc* 2014;(ii):308–18.
- [28] (a) Díaz-Ortiz A, de la Hoz A, Moreno A. Microwave-assisted synthesis and dynamic behaviour of *n*2,*n*4,*n*6-tris(1*h*-pyrazolyl)-1,3,5-triazine-2,4,6-triamines. *QSAR Comb Sci* 2005;24:649–59. <http://dx.doi.org/10.1002/qsar.200420116>.  
(b) Pinteá M, Fazekas M, Lameiras P, Cadis I, Berghian C, Silaghi-Dumitrescu I, et al. Serinolic amino-*s*-triazines: iterative synthesis and rotational stereochemistry phenomena as *n*-substituted derivatives of 2-aminopropane-1,3-diols. *Tetrahedron* 2008;64:8851–70. <http://dx.doi.org/10.1016/j.tet.2008.06.071>.
- [29] Alcázar J, Almena I, Begtrup M, de la Hoz A. Synthesis of 4-hydroxylamino-1-azabuta-1,3-dienes and their cyclization to 2-substituted pyrazole 1-oxides. *J Chem Soc Perkin Trans* 1995;1:2773–81. <http://dx.doi.org/10.1039/P19950002773>.
- [30] Sandström J. In *dynamic NMR spectroscopy*. New York: Academic Press; 1982.
- [31] (a) Miertus S, Scrocco E, Tomasi J. Electrostatic interaction of a solute with a continuum. a direct utilization of ab initio molecular potentials for the prevision of solvent effects. *J Chem Phys* 1981;55:117–29. [http://dx.doi.org/10.1016/0301-0104\(81\)85090-2](http://dx.doi.org/10.1016/0301-0104(81)85090-2).  
(b) Mennucci B, Tomasi J. Continuum solvation models: a new approach to the problem of solute's charge distribution and cavity boundaries. *J Chem Phys* 1997;106:5151–8. <http://dx.doi.org/10.1063/1.473558>.  
(c) Cammi R, Mennucci B, Tomasi J. Fast evaluation of geometries and properties of excited molecules in solution: a tamm-dancoff model with application to 4-dimethylaminobenzonitrile. *J Phys Chem A* 2000;104:5631–7. <http://dx.doi.org/10.1021/jp000156>.
- [32] Tang SW, Van Slyke SA. Organic electroluminescent diodes. *Appl Phys Lett* 1987;51:913–5. <http://dx.doi.org/10.1063/1.98799>.
- [33] Turro NJ. *Modern molecular photochemistry*. Sausalito, CA: University Science Books; 1991.
- [34] Adamo C, Jacquemin D. The calculations of excited-state properties with time-dependent density functional theory. *Chem Soc Rev* 2013;42:845–56. <http://dx.doi.org/10.1039/C2CS35394F>.
- [35] Le Guennic B, Jacquemin D. Taking up the cyanine challenge with quantum tools. *Acc Chem Res* 2015;48:530–7. <http://dx.doi.org/10.1021/ar500447q>.
- [36] (a) Drew A, Weisman JL, Head-Gordon M. Long-range charge-transfer excited states in time-dependent density functional theory require non-local exchange. *J Chem Phys* 2003;119:2943. <http://dx.doi.org/10.1063/1.1590951>.  
(b) Gritsenko O, Baerends EJ. Asymptotic correction of the exchange–correlation kernel of time-dependent density functional theory for long-range charge-transfer excitations. *J Chem Phys* 2004;121:655. <http://dx.doi.org/10.1063/1.1759320>.  
(c) Renz M, Theilacker K, Lambert C, Kaupp M. A reliable quantum-chemical protocol for the characterization of organic mixed-valence compounds. *J Am Chem Soc* 2009;131:16292–302. <http://dx.doi.org/10.1021/ja9070859>.
- (d) Wiggins P, Gareth Williams JA, Tozer DJ. Excited state surfaces in density functional theory: a new twist on an old problem. *J Chem Phys* 2009;131:091101. <http://dx.doi.org/10.1063/1.3222641>.
- [37] Peach MJG, Benfield P, Helgaker T, Tozer DJ. Excitation energies in density functional theory: an evaluation and a diagnostic test. *J Chem Phys* 2008;128:044118. <http://dx.doi.org/10.1063/1.2831900>.
- [38] (a) Wu CH, Chien CH, Hsu FM, Shihand PI, Shu CF. Efficient non-doped blue-light-emitting diodes incorporating an anthracene derivative end-capped with fluorene groups. *J Mater Chem* 2009;19:1464–70. <http://dx.doi.org/10.1039/B817031B>.  
(b) Kim YH, Jeong HC, Kim SH, Yang K, Kwon SK. High-purity-blue and high-efficiency electroluminescent devices based on anthracene. *Adv Funct Mater* 2005;15:1799–805. <http://dx.doi.org/10.1002/adfm.200500051>.
- [39] Meier H, Karpuk E, Christof Holst H. Star-shaped push-pull compounds having 1,3,5-triazine cores. *Eur J Org Chem* 2006;2609–17. <http://dx.doi.org/10.1002/ejoc.200600066>.
- [40] Zhao J, Ji S, Chen Y, Guo H, Yang P. Excited state intramolecular proton transfer (esipt): from principal photophysics to the development of new chromophores and applications in fluorescent molecular probes and luminescent materials. *Phys Chem Chem Phys* 2012;14:8803–17. <http://dx.doi.org/10.1039/c2cp23144a>.
- [41] (a) FluoProbes® Activated Cyanine Fluorophores for Labeling Biomolecules via their Amine Groups by NHS Acylation (Cyanine-NHS). (b) Fernando NT. *Novel near-infrared cyanine dyes for fluorescence imaging in biological systems*. Dissertation. Georgia State University; 2011.  
(c) Escobedo JO, Rusin O, Lim S, Strongin RM. NIR dyes for bioimaging applications. *Curr Opin Chem Biol* 2010;14:64–70. <http://dx.doi.org/10.1016/j.cbpa.2009.10.022>.
- [42] Jenekhe SA, Chen XL. Self-assembled aggregates of rod-coil block copolymers and their solubilization and encapsulation of fullerenes. *Science* 1998;279:1903–7. <http://dx.doi.org/10.1126/science.279.5358.1903>.
- [43] Smulders MMJ, Nieuwenhuizen MML, de Greef TFA, van der Schoff P, Schenning APHJ, Meijer EW. How to distinguish isodesmic from cooperative supramolecular polymerisation. *Chem Eur J* 2010;16:362–7. <http://dx.doi.org/10.1002/chem.200902415>.
- [44] Würthner F, Wortmann R, Matschiner R, Lukaszuk K, Meerholz K, Denardin Y, et al. Merocyanine dyes in the cyanine limit: a new class of chromophores for photorefractive materials. *Angew Chem Int Ed Eng* 1997;36:2765–8. <http://dx.doi.org/10.1002/anie.199727651>.
- [45] Kobayashi T, editor. *J-Aggregates*. Singapore: World Scientific; 1996.
- [46] Frisch MJ, Trucks GW, Schlegel HB, Scuseria GE, Robb MA, Cheeseman JR, et al. *Gaussian 09, revision D.01*. Wallingford CT: Gaussian, Inc.; 2009.
- [47] Davies IW, Marcoux JF, Wu J, Palucki M, Corley EG, Robbins MA, et al. An efficient preparation of vinamidinium hexafluorophosphate salts. *J Org Chem* 2000;65:4571–4. <http://dx.doi.org/10.1021/jo000159u>.
- [48] States DJ, Haberkorn RA, Ruben DJ. A two-dimensional nuclear overhauser experiment with pure absorption phase in four quadrants. *J Magn Reson* 1982;48:286–92. [http://dx.doi.org/10.1016/0022-2364\(82\)90279-7](http://dx.doi.org/10.1016/0022-2364(82)90279-7).
- [49] Williams ATR, Winfield SA, Miller JN. Relative fluorescence quantum yields using a computer-controlled luminescence spectrometer. *Analyst* 1983;108:1067–71. <http://dx.doi.org/10.1039/AN9830801067>.
- [50] Schnabel WJ, Rätz R, Kober E. The synthesis of substituted melams. *J Org Chem* 1962;27:2514–9. <http://dx.doi.org/10.1021/jo01054a050>.
- [51] Gazizov AS, Kharitonova NI, Buriilov AR, Pudovik MA, Sinyashin OG. One-pot synthesis of novel *s*-triazine-containing polyphenols and imidazotriazinium salts. *Monatsh Chem* 2013;144:1027–30. <http://dx.doi.org/10.1007/s00706-013-0939-1>.